

Two-dimensional semimetal in a wide HgTe quantum well: magnetotransport and energy spectrum

G. M. Minkov,^{1,2} A. V. Germanenko,² O. E. Rut,² A. A. Sherstobitov,^{1,2} S. A. Dvoretzki,³ and N. N. Mikhailov³

¹*Institute of Metal Physics RAS, 620990 Ekaterinburg, Russia*

²*Institute of Natural Sciences, Ural Federal University, 620000 Ekaterinburg, Russia*

³*Institute of Semiconductor Physics RAS, 630090 Novosibirsk, Russia*

(Dated: March 12, 2021)

The results of experimental study of the magnetoresistivity, the Hall and Shubnikov-de Haas effects for the heterostructure with HgTe quantum well of 20.2 nm width are reported. The measurements were performed on the gated samples over the wide range of electron and hole densities including vicinity of a charge neutrality point. Analyzing the data we conclude that the energy spectrum is drastically different from that calculated in framework of kP -model. So, the hole effective mass is equal to approximately $0.2m_0$ and practically independent of the quasimomentum (k) up to $k^2 \gtrsim 0.7 \times 10^{12} \text{ cm}^{-2}$, while the theory predicts negative (electron-like) effective mass up to $k^2 = 6 \times 10^{12} \text{ cm}^{-2}$. The experimental effective mass near $k = 0$, where the hole energy spectrum is electron-like, is close to $-0.005m_0$, whereas the theoretical value is about $-0.1m_0$.

I. INTRODUCTION

Two-dimensional (2D) systems based on gapless semiconductors such as HgTe represent unique object. A great variety of two-dimensional electron and hole systems based on this materials can be realized depending on the quantum well width (d) and content of cadmium in the well and barriers $\text{Hg}_{1-x}\text{Cd}_x\text{Te}$. It is well established now that the energy spectrum in single CdTe/HgTe/CdTe quantum well at $d = d_c \simeq 6.5 \text{ nm}$ is gapless¹ and close to the linear Dirac-like spectrum at small quasimomentum (k).² When thickness $d < d_c$ (i.e., when the HgTe quantum well is narrow) the energy spectrum is analogous to the spatially quantized spectrum of narrow gap semiconductor such as InSb. For thick HgTe layer, $d > d_c$, the quantum well is in inverted regime when the main electron subband of spatial quantization is formed at $k = 0$ from the heavy hole states.³

The energy spectrum and transport phenomena of 2D carriers in HgTe based structures were studied intensively last decade both experimentally^{4–10} and theoretically.^{2,11–13} The experimental data on the energy distance between the different 2D subbands at zero quasimomentum are in satisfactory agreement with the theory. Electron energy spectrum, electron effective mass and their dependence on the quantum well width are in agreement with the calculations also. As regards to the experimental data on the valence band energy spectrum, namely the value of bands overlapping, role of strain, effective masses at $k = 0$ and at large quasimomentum, they are discrepant and call for further investigation.

In this paper, we present the results of experimental study of the transport properties of the heterostructure with the HgTe quantum well with the inverted energy spectrum. The measurements were performed over wide range of electron and hole densities including the vicinity of the charge neutrality point (CNP) with nearly equal electron and hole densities. Analysis of experimental data brings us to the picture of the energy spectrum,

which drastically differs from the commonly accepted one.

II. EXPERIMENTAL

Our HgTe quantum wells were realized on the basis of HgTe/ $\text{Hg}_{1-x}\text{Cd}_x\text{Te}$ ($x = 0.58$) heterostructure grown by means of MBE on GaAs substrate with the (013) surface orientation.¹⁴ The nominal width of the quantum well was $d = 20.2 \text{ nm}$. The samples were mesa etched into standard Hall bars. To change and control the electron and hole densities (n and p , respectively) in the quantum well, the field-effect transistors were fabricated with the parylene as an insulator and aluminium as a gate electrode. The measurements were performed at the temperature of liquid helium in the magnetic field up to 8 T. All the data will be presented for $T = 1.35 \text{ K}$, unless otherwise specified. The architecture and the energy diagram of the structure investigated is shown in Fig. 1(a) and Fig. 1(b), respectively. The sketch of energy spectrum calculated within framework of the isotropic six-band kP -model with taking into account the lattice mismatch is presented in Fig. 1(c). One can see that h1-to-h2 interband distance at $k = 0$ is about 5 meV, the dispersion $E(k)$ in the valence band is non-monotonic.

III. RESULTS AND DISCUSSION

An overview of the magnetic field dependences of a transverse (ρ_{xy}) and longitudinal (ρ_{xx}) resistivity for different gate voltages (V_g) is presented in Fig. 2. It is seen that well defined quantum Hall plateaus of ρ_{xy} and minimum of ρ_{xx} are observed at electron ($V_g > 2 \text{ V}$) and hole ($V_g < -1 \text{ V}$) conductivity. Two peculiarities of these dependences should be pointed out. First, some minimum on the ρ_{xy} versus B and ρ_{xx} versus B dependences at $B = (4 - 6) \text{ T}$ [marked by arrows in Fig. 2(a) and in the

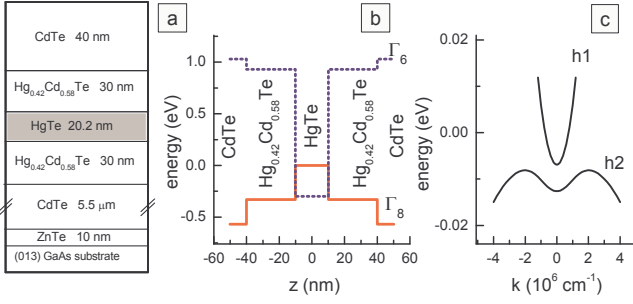


FIG. 1. (Color online) Architecture (a) and energy diagram (b) of the structure under investigation. (c) – The energy spectrum calculated within the framework of the isotropic six-band kP -model.

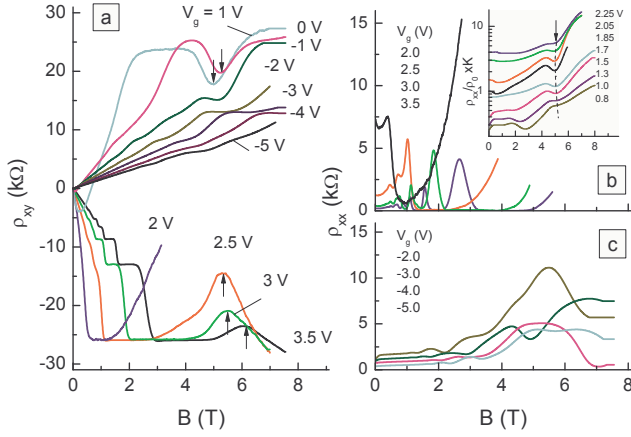


FIG. 2. (Color online) The magnetic field dependences of ρ_{xy} (a) and ρ_{xx} (b, c) measured for the different gate voltages. The minimum resulting from the crossing between the (h1, $n = 0$) and (h2, $n = 2$) Landau levels is marked by arrow (for more details, see Section IV). The inset in (b) illustrates the weak sensitivity of the minimum position to the gate voltage near the charge neutrality point, $V_g \simeq 1.8$ V.

inset in Fig. 2(b)] is observed. Its position only slightly depends on V_g within the gate voltage range from 3.0 V to 0.8 V.

Second, the alternative sign Hall resistivity ρ_{xy} , negative at low magnetic fields $B < (0.1 - 0.5)$ T and positive at higher ones [see Fig. 3(a)], is observed within the gate voltage range $(-3 \dots +1.8)$ V. Such behavior of ρ_{xy} accompanied by strong positive magnetoresistivity [Fig. 3(b)] shows that two types of carriers, electrons and holes, take part in the conductivity within this gate voltage range. The Hall densities of electrons and holes found as $1/eR_H(B)$ at $B = 0.05$ T and $B = 2$ T, respectively, are plotted against the gate voltage in Fig. 4. Excepting the gate voltage range from 0 V to 2 V, the data points fall on a straight line with the slope $-5.5 \times 10^{10} \text{ cm}^{-2} \text{ V}^{-1}$, which is close to $-1/eC$, where $C = 9.1 \text{ nF/cm}^2$ is the capacity between the 2D gas and gate electrode measured on the same structure.¹⁵ So, beyond the range

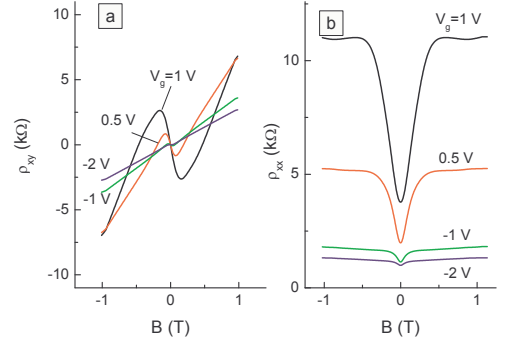


FIG. 3. (Color online) The low-magnetic-field dependences of ρ_{xy} (a) and ρ_{xx} (b) measured for $B < 1$ T at different gate voltages near the charge neutrality point.

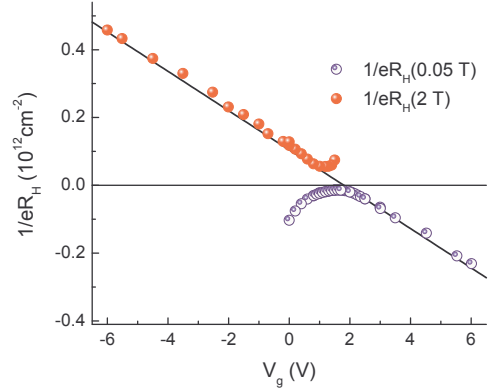


FIG. 4. (Color online) The gate voltage dependence of $1/eR_H(0.05 \text{ T})$ and $1/eR_H(2 \text{ T})$. The line is the charge density in the quantum well calculated as $C(1.8 \text{ V} - V_g)/e$, where C is the capacity between the gate electrode and quantum well measured experimentally, $C = 9.1 \text{ nF/cm}^2$.

$V_g \simeq (0 \dots 2) \text{ V}$, $-1/eR_H(0.05 \text{ T})$ and $1/eR_H(2 \text{ T})$ give the electron and hole densities, n and p , respectively. The gate voltage $V_g = 1.8 \text{ V}$, at which the straight line crosses zero, corresponds to CNP.

It is clear that both the peculiarities may result from specific features of the energy spectrum of 2D carriers in the structures under study. There are several papers^{4-6,10,16,17} on the energy spectrum of electrons and holes in HgTe quantum wells with approximately the same width of the well. However, the energy spectrum, especially of the valence band, is not understood up to now. Therefore, let us start from analysis of the Shubnikov-de Haas (SdH) oscillations.

The positions of the oscillation minima are plotted in the (B, V_g) plane in Fig. 5. This figure resembles a fan-chart showing the energies of Landau levels as a function of magnetic field. However, it should be noted that the gate voltage, rather than the energy is plotted in the vertical axis. Only in the case when the carrier effective mass does not depend on the energy, the energy varies in direct proportion with V_g , $E \propto CV_g/e\nu$, where ν is density of

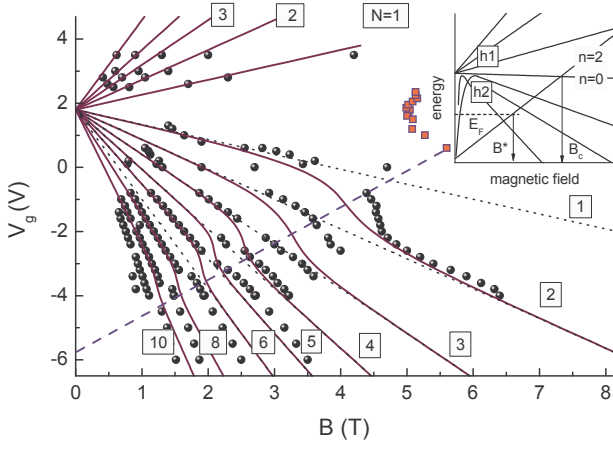


FIG. 5. (Color online) The fan-chart diagram showing the positions of the minima in ρ_{xx} versus B dependence. Symbols are the experimental results, the squares correspond to the minima labeled in Fig. 2 by arrows. The dashed line is the B dependence of the gate voltage corresponding to a crossing of the Landau level ($h2$, $n = 2$) with the Fermi level. Solid lines show the expected minima positions found as $V_g^N = \pm eBN/5.5 \times 10^{10} h + 1.8$ V (above dashed line) and $V_g^N = -eB(N + 1)/5.5 \times 10^{10} h + 1.8$ V (below dashed line). The inset is schematic dispersion of Landau levels.

states. It is clearly seen that the points laying above the dashed line fall on the straight lines, which are extrapolated to $V_g = (1.8 \pm 0.1)$ V when $B \rightarrow 0$ corresponding to CNP. Just such the behavior should be observed when the variation of density of carriers with V_g is determined by the geometrical capacity only.¹⁵ The behavior of ρ_{xx} minima near the dashed line will be discussed below.

At hole density higher than 10^{11} cm^{-2} that corresponds to $V_g < 0$ V, one can find the range of low magnetic field, where the spin-unsplit SdH oscillations are observed [for example see Fig. 6(b)]. Fitting the temperature dependence of oscillation amplitude to the Lifshitz-Kosevich formula,¹⁸ we have found the hole effective mass. We succeeded in such analysis within the density range $(1 \dots 4) \times 10^{11} \text{ cm}^{-2}$. The results are plotted in Fig. 6(a). One can see that the hole effective mass is equal to $m_h = (0.2 \pm 0.05) m_0$ and only slightly increases with the increasing hole density. Note that the hole density found from SdH oscillations is close to that found as $1/eR_H(2 \text{ T})$.

Let us compare this result with the result of the conventional calculation performed within framework of isotropic envelop function approximation based on six-band kP -Hamiltonian. Because the valence band spectrum noticeably depends on the strain, we present in Fig. 6 the E versus k and m_h versus k dependences calculated for two cases: with and without taking into account the strain caused by the HgTe and $\text{Hg}_{1-x}\text{Cd}_x\text{Te}$ lattice mismatch. The strain effect is characterized by the quantity $2\Delta_\epsilon$, which is the splitting of Γ_8 band at $k = 0$ in the bulk HgTe. The estimate for our case, $x = 0.58$,

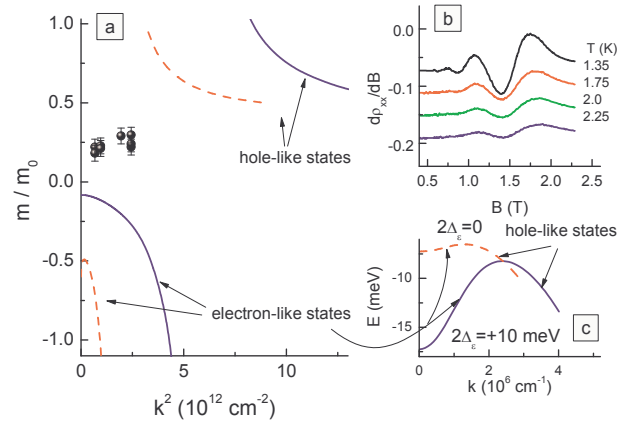


FIG. 6. (Color online) (a) – The hole effective mass plotted against the k^2 value as obtained experimentally (symbols) and calculated theoretically from six-band kP -model with and without taking into account the lattice mismatch (the solid and dashed curves, respectively). (b) – An example of the SdH oscillations measured for $V_g = 0.25$ V ($p = 1.05 \times 10^{11} \text{ cm}^{-2}$) at different temperatures. (c) – The dispersion for the upper hole subband $h2$ calculated from six-band kP -model with and without taking into account the lattice mismatch (the solid and dashed curves, respectively).

gives $2\Delta_\epsilon \simeq 10$ meV. It is seen that the theory for both cases predicts so called “Mexican hat” hole energy spectrum, characterized by the electron-like dispersion $E(k)$ with the positive curvature near $k = 0$. It is significant that the hole effective mass calculated theoretically is negative up to $k^2 \simeq 2 \times 10^{12} \text{ cm}^{-2}$ or $\simeq 6 \times 10^{12} \text{ cm}^{-2}$ depending on the strain. Experimentally, m_h is positive when $k^2 \gtrsim 0.7 \times 10^{12} \text{ cm}^{-2}$. This conclusion follows immediately from the fact that the oscillation minima at $V_g < 0$ shift to the more negative V_g with the growing magnetic field (Fig. 5). Note that found values of m_h are close to those found from cyclotron resonance.¹⁹ Thus, experimentally found hole effective mass at low k differs drastically from the calculated one to the extent that they are different in sign.

The electron effective mass m_e measured by the same way for $n = (0.6 \dots 1.5) \times 10^{11} \text{ cm}^{-2}$ is equal to $(0.02 \pm 0.005) m_0$ that also coincides with the result obtained in the cyclotron resonance experiments.¹⁹ Such the value of m_e is something less than the calculated one, which is equal to $0.028 m_0$ and practically independent of the density up to $n = 3 \times 10^{11} \text{ cm}^{-2}$.

The results discussed above do not give information on the energy spectrum at small k values, $k^2 \lesssim 0.7 \times 10^{12} \text{ cm}^{-2}$, and on overlapping value of the conduction and valence bands. Such information can be obtained from analysis of the low-field magnetoresistivity and Hall effect near CNP.

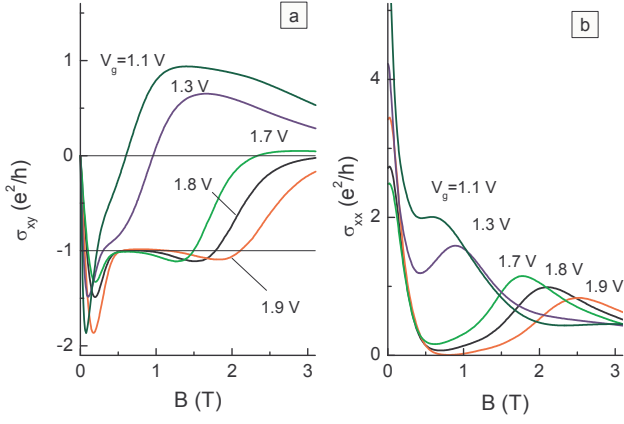


FIG. 7. (Color online) The magnetic field dependences of σ_{xy} (a) and σ_{xx} (b) for several gate voltages near CNP.

IV. TRANSPORT NEAR CNP. TWO TYPES OF CHARGE CARRIERS

The detailed measurements at low magnetic field show, that over the gate voltage range $(-6 \dots 1.7)$ V when the electron density is less than $(1.0 \dots 1.5) \times 10^{10} \text{ cm}^{-2}$ and the hole density is less than $5 \times 10^{11} \text{ cm}^{-2}$, the Hall resistivity ρ_{xy} is strongly nonlinear in the magnetic field at $B < (0.1 \dots 0.5)$ T insofar that it changes the sign [see Fig. 3(a)]. The large positive magnetoresistivity is observed within this magnetic field range [Fig. 3(b)]. Both these facts strongly suggest that two types of carriers, electrons and holes, take part in transport, i.e., the system is in two type carrier conductivity (TTCC) regime. It is more instructive for this case to plot the magnetic field dependence of σ_{xy} and σ_{xx} instead of ρ_{xx} and ρ_{xy} because just the conductivity tensor components are additive. These dependences for the different gate voltages are plotted in Fig. 7. It is worth noting that at $V_g = 1.7$ V σ_{xy} changes the sign from electron to hole one at $B = 2.2$ T therewith the last electron plateau of σ_{xy} (with $\sigma_{xy} = e^2/h$) is observed at lower magnetic field, $B = (0.5 - 1.5)$ T. Such unusual quantum Hall effect determined by minority carriers, which are electrons in this situation, is observed down to $V_g = 1.4$ V.

Let us analyze the results relating to the gate voltage range where two types of carriers take part in the transport in more detail. There are several physical reasons for such regime: (i) the existence of the edge states,^{2,8,20} which give the electron contribution to the conductivity, while the 2D gas is of hole type; (ii) existence of the electron and hole drops due to potential fluctuations; (iii) the overlapping between the conduction and valence bands following from the standard kP -model.¹⁰

If the edge states result in the conductivity by two types of carriers, their relative contribution can be estimated from the value of step-like drop $\Delta\sigma = 1/\rho_{xx}(0.5 \text{ T}) - 1/\rho_{xx}(0)$ evident in the $1/\rho_{xx}$ versus B dependence (see inset in Fig. 8). Because this drop should

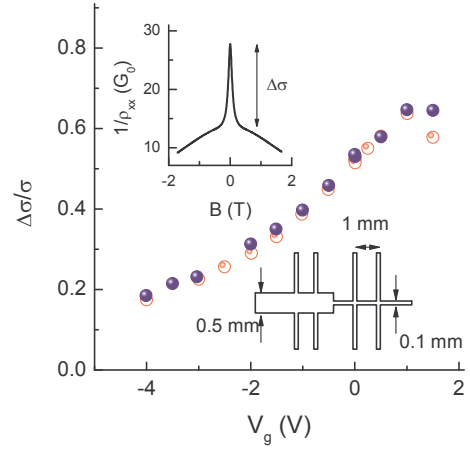


FIG. 8. (Color online) The relative value of the drop in the $1/\rho_{xx}$ dependence plotted as a function of the gate voltage for the wide (open symbols) and narrow (solid symbols) parts of the samples shown in the sketch. The inset is $1/\rho_{xx}$ plotted as a function of the magnetic field. Arrow indicates the drop $\Delta\sigma$.

be inversely proportional to the channel width for this mechanism, we have measured magnetoresistance of wide (0.5 mm) and narrow (0.1 mm) parts of the Hall bar sketched in Fig. 8. As seen from Fig. 8 the relative drop values, $\Delta\sigma/\sigma$, are practically identical for the wide and narrow parts of the bar. It means that the edge states in the structures investigated do not responsible for the two types carriers conductivity regime.

Another possible reason of two type charge carrier conductivity is that the large long-range fluctuation potential leads to existence of n (or p) type droplets in the p (or n) type matrix. Due to large transparency of p - n junction in the structure with inverted energy spectrum, such medium will demonstrate features typical for systems with two types of carriers. The upper limit of the fluctuation potential amplitude can be estimated from the value of the Dingle temperature (T_D). As follows from analysis of the SdH oscillations its value does not exceed 1 meV. So, this mechanism may account for two type carrier conductivity within narrow gate voltage range only, which can be estimated as $\Delta V_g \simeq \nu_h T_D (dn/dV_g)^{-1} \simeq 1$ V ($\nu_h = m_h/\pi\hbar^2$ is the hole density of states, $m_h = 0.2m_0$). Experimentally, this regime occurs within much wider range of V_g : from -6 V to $+1.7$ V.

Thus, we assume that TTCC regime arises from bands overlapping due to non-monotonic “Mexican hat” energy spectrum of the upper valence subband and thus the data can be analyzed in the framework of model of laterally homogeneous 2D gas. It is naturally in this case to use the classical hand-book formulae for two types of carriers to fit the magnetic field dependences of ρ_{xx} and R_H (see, e.g., Ref. 21). Such the fitting procedure has been performed at low magnetic field, $B < 0.3$ T, with the use of densities and mobilities of electrons and holes as the fitting parameters under assumption that they are

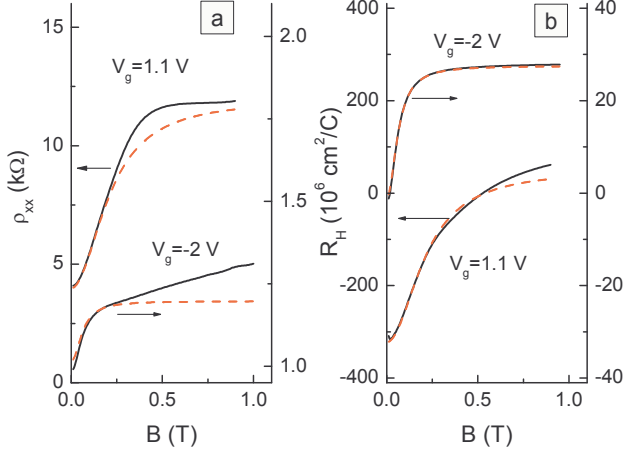


FIG. 9. (Color online) The magnetic field dependences of ρ_{xx} (a) R_H (b). The solid curves are measured experimentally, the dashed lines are the results of the best fit to the classical formula for TTCC regime.

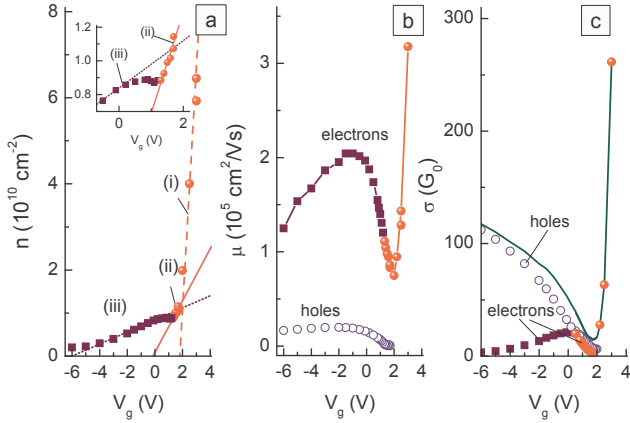


FIG. 10. (Color online) (a) and (b) – The gate voltage dependences of the electron density and mobility, respectively, obtained at $V_g < 1.7$ V within framework of standard TTCC model. (c) – The partial electron and hole conductivities plotted against the gate voltage. The parameters of electrons for $V_g > 1.8$ V for all the panels are obtained as follows: $n = 1/e|R_H(0.03 \text{ T})|$, $\mu_e = |R_H(0.03 \text{ T})|\sigma$.

independent of magnetic field. The results of the best fit for $V_g = 1.1$ V and $V_g = -2$ V are shown in Fig. 9. It is seen that this simple model quite well describes both dependences, $\rho_{xx}(B)$ and $R_H(B)$. The gate voltage dependence of electron density found by this manner at $V_g < 1.7$ V is plotted in Fig. 10(a) [points at $V_g > 1.8$ V are obtained as $1/e|R_H(0.03 \text{ T})|$]. It is necessary to stress that electron contribution to the conductivity occurs down to the very large negative gate voltages, $V_g \simeq -6$ V, when the hole density becomes about $5 \times 10^{11} \text{ cm}^{-2}$ (see Fig. 4).

Let us consider the V_g dependence of density in greater detail. It is rather complicated as evident from Fig. 10(a). There are three V_g intervals distinguished

by the slopes. (i) At $V_g > 1.8$ V, when the Fermi level lies in the conduction band, the electron density decreases with decreasing V_g with the rate $\Delta n/\Delta V_g$ of about $5.5 \times 10^{10} \text{ cm}^{-2} \text{ V}^{-1}$. (ii) At $V_g = (1.0 \dots 1.7)$ V, the rate is about ten times less, than that at $V_g > 1.8$ V, $\Delta n/\Delta V_g \simeq 6.0 \times 10^9 \text{ cm}^{-2} \text{ V}^{-1}$ [see inset in Fig. 10(a)]. Quite apparently this feature results from the fact that the holes appear at $V_g \simeq 1.8$ V, and the rate of decrease of the Fermi energy is already determined by the hole density of states, which is ten times larger than the electron one: $dE_F/dV_g|_{V_g > 1.8 \text{ V}} = (1 + m_h/m_e) dE_F/dV_g|_{V_g < 1.8 \text{ V}}$. Thus, extrapolating the n versus V_g plot to $n = 0$ one obtains that the electrons of the conduction band have to disappear at $V_g \approx 0$ V [see the solid line in Fig. 10(a) and the inset in it]. (iii) At $V_g = (-6 \dots +1)$ V, the electron contribution to the conductivity remains essential, as it follows from analysis of the magnetic field dependences of R_H and ρ_{xx} , despite the fact that the electrons in the conduction band are expected to disappear at $V_g \approx 0$ V. The data points in this range fall on the straight line with the slope $\Delta n/\Delta V_g \simeq 1.5 \times 10^9 \text{ cm}^{-2} \text{ V}^{-1}$.

We focus now attention on the gate voltage dependence of the electron mobility [Fig. 10(b)]. As clearly seen it is nonmonotonic; sharp minimum is evident near $V_g \simeq 1.8$ V. At $V_g > 1.8$ V, when the conductivity is determined by the conduction band electrons and the holes in the valence band are absent, the mobility decreases with the decreasing gate voltage. This is natural because the decrease of the electron density and hence the electron energy leads to the increase of scattering probability independently of that short- or long-range scattering potential determines the mobility. The increase of electron mobility with decreasing V_g at $V_g < 1.8$ V, where the electron density carries on decreasing, seems strange at first sight. However it can be explained by holes appeared at these gate voltages, which screen the potential of scatterers effectively due to the large effective mass. The authors of Ref. 22 who observed analogous behavior of the electron mobility come to the same conclusion.

As was discussed above, the contribution of the conduction band electrons to the conductivity has to disappear at $V_g \approx 0$ V so presence of electron contribution up to the large negative V_g seems surprising. Broadly speaking, shunting conductivity channels of technological nature can make such a type of contribution. They can be located either above the quantum well or below it. If such channels are situated above the well, i.e., between the quantum well and the gate electrode, they should reveal themselves in the capacitance measurements. However, no peculiarities in the voltage-capacity characteristics caused by the depletion of these channels were observed in our experiments. Besides, the contribution of the channels to the conductivity has to be enhanced with the increasing positive gate voltage due to the increase of electron density in these channels. However, as Fig. 10(c) shows the electron contribution to the conductivity has a maximum at $V_g \simeq 0$ V and decreases with the increas-

ing positive gate voltage. If the shunting channels are located below the well, their contribution should disappear at the negative voltage applied to the back gate electrode. Our measurements performed on the back-gated samples show that the voltage applied to the back- and top gate electrodes changes the magnetic field dependences of R_H and ρ_{xx} analogously. Thus no conducting channels exist above or below the quantum well.

It remains to assume that the electron contribution at $V_g < 0$ V is caused by carriers in the well, namely, by the holes with electron-like energy spectrum characterized by the negative effective mass in vicinity of $k = 0$. Thus, such data interpretation leads to the energy spectrum sketched in Fig. 11. Qualitatively, it is close to the calculated one, however quantitative difference is significant. The conduction and valence bands are overlapped. The value of overlapping (ΔE_{ovrl}) can be estimated from the value of the electron density at the gate voltage corresponding to appearance of the hole contribution to the conductivity, $V_g \simeq 1.8$ V (see Fig. 10). As seen from this figure $n \sim 1 \times 10^{10} \text{ cm}^{-2}$ at $V_g \simeq 1.8$ V that gives $\Delta E_{\text{ovrl}} \simeq n/\nu_e \sim 1$ meV if one uses the experimental value of electron effective mass $m_e = 0.02m_0$ to calculate the electron density of states ν_e .

Experimentally, the hole energy spectrum is monotonic at $p \gtrsim 10^{11} \text{ cm}^{-2}$ that corresponds to $k = (2\pi p)^{1/2} \gtrsim 8 \times 10^5 \text{ cm}^{-1}$. This conclusion follows immediately from the two facts. First, the hole Hall density $p = 1/eR_H$ is close to that found from SdH oscillations. Second, the peaks of SdH oscillations are shifted to the higher magnetic field when the gate voltage becomes more negative (see Fig. 5). For $k < (7-8) \times 10^5 \text{ cm}^{-1}$, the hole energy spectrum is electron-like; there is narrow minimum in the dispersion $E(k)$. The depth of this minimum can be easily estimated from the hole density wherein the electron contribution disappears: $\Delta = p|_{n=0}/\nu_h$, where $p|_{n=0}$ is the hole density for the gate voltage $V_g \simeq -6$ V [see Fig. 10(a)]. With the use of experimental value of the hole effective mass, $m_h = 0.2m_0$, and $p|_{n=0} = p(V_g = -6 \text{ V}) \simeq (4 \dots 5) \times 10^{11} \text{ cm}^{-2}$ (see Fig. 4), one obtains $\Delta \simeq 5$ meV. The effective mass of electron-like states of the valence band is about $m_{e-l} \simeq -0.005m_0$. This estimate is obtained from the depth of minimum Δ and from the amount of electron-like states, $\simeq 1 \times 10^{10} \text{ cm}^{-2}$, estimated as n in the region $V_g = (0 \dots 1)$ V [see Fig. 10(a)]: $|m_{e-l}| = \pi \hbar^2 n(V_g = 1 \text{ V})/\Delta$. Since three types of carriers take part in the transport at $V_g = (0 \dots 1)$ V, the n values at these gate voltages are obtained with considerably low accuracy. Therefore, this estimate for m_{e-l} should be considered as rough enough. In Fig. 11, we reconstruct the energy spectrum using the parameters m_e , m_h , m_{e-l} , Δ and ΔE_{ovrl} and compare it with the spectrum calculated in framework of the kP -model. One can see that E versus k dependence in conduction band is close to the theoretical one. The difference between the dispersion curves $E(k)$ for the valence band is crucial.

We perceive that strong difference between the calculated and reconstructed spectra indicates that discussion

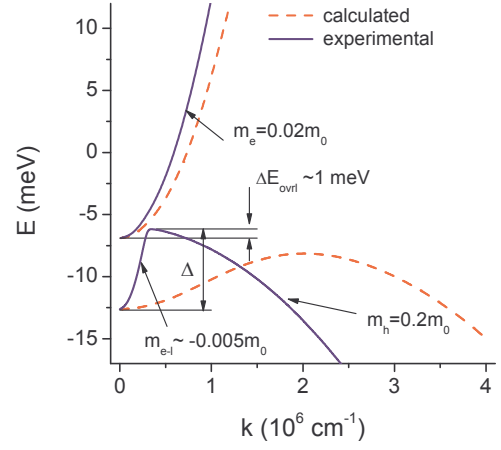


FIG. 11. (Color online) The dispersion $E(k)$ reconstructed from the data analysis as described in the text (solid lines) and calculated within framework of isotropic six-band kP -model (dashed lines).

of alternative approaches to the interpretation of the data is required. This will be done below. Now let us examine the additional arguments in favor of the energy spectrum depicted in Fig. 11. They can be obtained from analysis of the data obtained in strong magnetic field.

As noted above, the experimental dependences $\rho_{xy}(B)$ and $\rho_{xx}(B)$ exhibit some peculiarities at the gate voltages near CNP [in Figs. 2(a) and 2(b), they are marked by the arrows]. The position of this minimum in the (B, V_g) coordinates is shown in Fig. 5 by squares. Its origin directly relates to specific features of the magnetic field quantization of the energy spectrum in the quantum well with inverted spectrum.²³ There are two singular Landau levels responsible for that [see Fig. 1 in Ref. 23 and the inset in Fig. 5]. One of them is the lowest level (h1, $n = 0$) of the conduction band. Due to complex nature of the band structure, its energy linearly decreases with increasing magnetic field, while the other Landau levels of the conduction band increase their energies as it takes place in usual system. The second singular Landau level is the singular level (h2, $n = 2$) of the valence band, which starts at $B = 0$ from the energy of h2 branch at $k = 0$ and shifts upward with the increasing B . Unusual behavior of these levels leads to a crossing of the conduction- and valence band states at the critical value of the magnetic field, $B = B_c$. The behavior of the crossing point with the change of the quantum well width is investigated in Ref. 8. If one extrapolates the calculation results⁸ to $d = 20$ nm, we obtain $B_c \simeq (4-5)$ T, which is close to position of the peculiarities evident in the ρ_{xx} - and ρ_{xy} versus B dependences.

Thus, for the case when n is slightly larger than p , the Fermi level lies in the Landau level (h1, $n = 0$) at $B \lesssim B_c$, while at higher magnetic field, $B \gtrsim B_c$, it occurs in the Landau level (h2, $n = 2$) resulting in switching of the electron ground state and in the peculiarity of ρ_{xx} and ρ_{xy} . Existence of such switching was discussed in

recent paper.²⁴

The level (h2, $n = 2$) reveals itself not only at low charge carrier density. Really, inspection of Fig. 5 shows that the data points located above the dashed line fall on the straight lines, which are well extrapolated to the common point $V_g \simeq 1.8$ V at $B = 0$. Their positions can be estimate from simple relation $n, p(V_g) = \pm BN/h$, where N is the number of occupied Landau levels. Because experimentally $n + p \simeq -5.5 \times 10^{10} (V_g - 1.8 \text{ V}), \text{ cm}^{-2}$ (see Fig. 4), we obtain for V_g^N : $V_g^N = \pm eBN/5.5 \times 10^{10} h + 1.8$ V. The solid lines in Fig. 5 are drawn according to this equation. It is seen that the separation between the data points corresponding to $N = 2$ and 3 is well resolved while the points with $N = 4$ and 5, $N = 6$ and 7, and so forth, are merged. The points below the dashed line turn out to be shifted from the lines. The reason is clear. When the level (h2, $n = 2$) increasing its energy with the growing magnetic field crosses the Fermi level at magnetic field $B = B^*$ (see inset in Fig. 5), the number of Landau levels occupied by holes becomes larger on 1 so that the positions of minima below the dashed line in Fig. 5 should be described by $V_g^N = -eB(N+1)/5.5 \times 10^{10} h + 1.8$ V and, thus, the oscillations turn out to be shifted (see solid lines in Fig. 5). Thus, by and large this model describes the behavior of the oscillation minima rather well. Some discrepancy is not surprising because this simple model is valid when the overlapping between the Landau levels is small, while the experimental data were obtained within the wide magnetic field range involving both the Shubnikov-de Haas oscillations and the quantum Hall ranges.

The main conclusion, which follows from this consideration and from Fig. 5 is that the Landau level (h2, $n = 2$) at $B \rightarrow 0$ crosses the Fermi level at $V_g \simeq -6$ V, when the hole density is about $4.5 \times 10^{11} \text{ cm}^{-2}$. It means that the Fermi level lies below the top of the valence band for a distance of ~ 5 meV. This value is consistent with that estimated from the hole density at the gate voltage corresponding to disappearance of the electron contribution to the conductivity, that supports the energy spectrum presented in Fig. 11 as well.

Let us now discuss alternative interpretations of data. Analogous heterostructures were investigated in Refs. 10, 25–27. Partially, our results and results reported in these papers are overlapping. It concerns in particular the value of the hole effective mass,²⁷ existence of electron contribution to the conductivity up to the hole density $(4-5) \times 10^{11} \text{ cm}^{-2}$.¹⁰ To interpret the results, the authors of Refs. 25 and 26 suggest that there is an overlap by about 5 meV of the conduction band minimum at $k = 0$ with two symmetrical maxima of the valence band located at $k \neq 0$ in the direction [031] characterized by the effective masses close to $0.2 m_0$. This picture agrees well with the value of electron density $n \simeq (4-5) \times 10^{10} \text{ cm}^{-2}$ (it is four-to-five times higher than that in our case), at which the hole contribution to the conductivity appears in samples investigated in Ref. 26. However this model of the energy spectrum is in conflict with the fact that the

hole density found from the period of SdH oscillations coincides with that obtained from the Hall effect. Because the valence band has two maxima in the spectrum, the hole density obtained from the SdH experiments should be twice as small as the Hall density. To resolve this contradiction the authors¹⁰ assume that the spectrum is split by spin-orbit interaction due to asymmetry of the quantum well. It is, however, strange that this effect does not reveal itself in SdH oscillations. The results^{25,26} can be understood in framework of our model, where the lines of constant energy are (nearly) circle centered at $k = 0$. However our results cannot be interpreted within framework of the model suggested in Refs. 25 and 26. First, the hole contribution to the conductivity in our samples appears at the electron density of about $1 \times 10^{10} \text{ cm}^{-2}$ instead of $5 \times 10^{10} \text{ cm}^{-2}$ in Ref. 26. This corresponds to the overlap value of about 1 meV instead of 5 meV. Second, the spin-orbit splitting in our samples is evident in SdH effect at $n \gtrsim 2 \times 10^{11} \text{ cm}^{-2}$ and $p \gtrsim 4 \times 10^{11} \text{ cm}^{-2}$. At lower densities its value is estimated as 1 meV or less, i.e., the valence band can be considered as unsplit one under our experimental conditions.

Thus, our results and their interpretation lead us to the conclusions on the energy spectrum of the HgTe quantum well which are inconsistent with that obtained in framework of traditional kP -model. A most surprising result is existence of narrow electron-like pit in the center of the valence band with the depth of about 5 meV characterized by the very low effective mass $|m_{e-l}| \simeq 0.005 m_0$.

V. CONCLUSION

We have studied the transport phenomena in HgTe single quantum well with inverted energy spectrum. Consistent analysis of the magnetic field dependences of the magnetoresistivity, the Hall coefficient, and the SdH effect in the gated samples carried out over the wide range of the electron and hole densities including the charge neutrality point leads us to the conclusion that the structure of the top of the valence band is drastically different from that predicted in framework of standard kP -approach. We obtain that the hole effective mass is equal to approximately $0.2 m_0$ at $k \gtrsim 0.7 \times 10^{12} \text{ cm}^{-2}$ and practically independent of the hole density, while the theory predicts negative (electron-like) effective mass up to $k^2 \simeq 6 \times 10^{12} \text{ cm}^{-2}$. The experimentally obtained effective mass near $k = 0$, where the spectrum is electron-like, is close to $-0.005 m_0$, whereas the theory predicts the value less than $-0.1 m_0$. All this indicates that the further experimental and theoretical investigations are needed to find the answer to the question of whether the standard kP model adequately describes the energy spectrum of wide HgTe based single quantum well.

ACKNOWLEDGMENTS

This work has been supported in part by the RFBR (Grant Nos. 10-02-91336, 10-02-00481, and 12-02-00098).

-
- ¹ L. G. Gerchikov and A. Subashiev, Phys. Stat. Sol. (b) **160**, 443 (1990).
- ² B. A. Bernevig, T. L. Hughes, and S.-C. Zhang, Science **314**, 1757 (2006).
- ³ M. I. D'yakonov and A. Khaetskii, Zh. Eksp. Teor. Fiz. **82**, 1584 (1982), [Sov. Phys. JETP **55**, 917 (1982)].
- ⁴ G. Landwehr, J. Gerschütz, S. Oehling, A. Pfeuffer-Jeschke, V. Latussek, and C. R. Becker, Physica E **6**, 713 (2000).
- ⁵ X. C. Zhang, A. Pfeuffer-Jeschke, K. Ortner, C. R. Becker, and G. Landwehr, Phys. Rev. B **65**, 045324 (2002).
- ⁶ K. Ortner, X. C. Zhang, A. Pfeuffer-Jeschke, C. R. Becker, G. Landwehr, and L. W. Molenkamp, Phys. Rev. B **66**, 075322 (2002).
- ⁷ X. C. Zhang, K. Ortner, A. Pfeuffer-Jeschke, C. R. Becker, and G. Landwehr, Phys. Rev. B **69**, 115340 (2004).
- ⁸ M. König, S. Wiedmann, C. Brüne, A. Roth, H. Buhmann, L. W. Molenkamp, X.-L. Qi, and S.-C. Zhang, Science **318**, 766 (2007).
- ⁹ G. M. Gusev, Z. D. Kvon, O. A. Shegai, N. N. Mikhailov, S. A. Dvoretzky, and J. C. Portal, Phys. Rev. B **84**, 121302 (2011).
- ¹⁰ Z. D. Kvon, E. B. Olshanetsky, E. G. Novik, D. A. Kozlov, N. N. Mikhailov, I. O. Parm, and S. A. Dvoretzky, Phys. Rev. B **83**, 193304 (2011).
- ¹¹ G. Tkachov and E. M. Hankiewicz, Phys. Rev. B **84**, 035444 (2011).
- ¹² J. W. Nicklas and J. W. Wilkins, Phys. Rev. B **84**, 121308 (2011).
- ¹³ P. M. Ostrovsky, I. V. Gornyi, and A. D. Mirlin, Phys. Rev. B **86**, 125323 (2012).
- ¹⁴ N. N. Mikhailov, R. N. Smirnov, S. A. Dvoretzky, Y. G. Sidorov, V. A. Shvets, E. V. Spesivtsev, and S. V. Rykhlit-ski, Int. J. Nanotechnology **3**, 120 (2006).
- ¹⁵ The capacity measured is practically independent of the gate voltage over the entire V_g range. Only one percent variation of C resulting from the finite value of compressibility of the electron gas is evident at $V_g \approx 1.8$ V.
- ¹⁶ X. C. Zhang, A. Pfeuffer-Jeschke, K. Ortner, V. Hock, H. Buhmann, C. R. Becker, and G. Landwehr, Phys. Rev. B **63**, 245305 (2001).
- ¹⁷ M. Orlita, K. Masztalerz, C. Faugeras, M. Potemski, E. G. Novik, C. Brüne, H. Buhmann, and L. W. Molenkamp, Phys. Rev. B **83**, 115307 (2011).
- ¹⁸ I. M. Lifshits and A. M. Kosevich, Zh. Eksp. Teor. Fiz. **29**, 730 (1955), [Sov. Phys. JETP **2**, 636 (1956)].
- ¹⁹ Z. D. Kvon, S. N. Danilov, D. A. Kozlov, C. Zoth, N. N. Mikhailov, S. A. Dvoretzky, and S. D. Ganichev, Pis'ma Zh. Eksp. Teor. Fiz. **94**, 895 (2011), [JETP Letters **94**, 816 (2011)].
- ²⁰ A. Roth, C. Brüne, H. Buhmann, L. W. Molenkamp, J. Maciejko, X.-L. Qi, and S.-C. Zhang, Science **325**, 294 (2009).
- ²¹ F. J. Blatt, *Physics of electronic conduction in solids* (McGraw-Hill Inc., US, 1968) p. 446.
- ²² E. Olshanetsky, Z. Kvon, N. Mikhailov, E. Novik, I. Parma, and S. Dvoretzky, Solid State Commun. **152**, 265 (2012).
- ²³ M. Schultz, U. Merkt, A. Sonntag, U. Rössler, R. Winkler, T. Colin, P. Helgesen, T. Skauli, and S. Løvold, Phys. Rev. B **57**, 14772 (1998).
- ²⁴ O. E. Raichev, G. M. Gusev, E. B. Olshanetsky, Z. D. Kvon, N. N. Mikhailov, S. A. Dvoretzky, and J. C. Portal, Phys. Rev. B **86**, 155320 (2012).
- ²⁵ Z. D. Kvon, E. Olshanitsky, D. A. Kozlov, N. N. Mikhailov, and S. A. Dvoretzky, Pis'ma Zh. Eksp. Teor. Fiz. **87**, 588 (2008), [JETP Lett. **87**, 502 (2008)].
- ²⁶ E. Olshanitsky, Z. D. Kvon, M. V. Entin, L. I. Magarill, N. N. Mikhailov, I. O. Parm, and S. A. Dvoretzky, Pis'ma Zh. Eksp. Teor. Fiz. **89**, 338 (2009), [JETP Lett. **89**, 290 (2009)].
- ²⁷ D. A. Kozlov, Z. D. Kvon, N. N. Mikhailov, S. A. Dvoretzky, and J. C. Portal, Pis'ma Zh. Eksp. Teor. Fiz. **93**, 186 (2011), [JETP Lett. **93**, 170 (2011)].